Sains Malaysiana 52(8)(2023): 2407-2418
http://doi.org/10.17576/jsm-2023-5208-17

Composite of Titanium Dioxide Nanotube and Cobalt Sulfide for Photoelectrochemical Application

(Komposit Nanotiub Titanium Dioksida dan Kobalt Sulfida untuk Aplikasi Fotoelektrokimia)

MUSTAFID AMNA RAMBEY[1], SITI NURUL FALAEIN MORIDON[1], KHUZAIMAH ARIFIN[1,2,*], LORNA JEFFERY MINGGU[1] & MOHAMMAD B. KASSIM[1,3]

[1]Fuel Cell Institute, Universiti Kebangsaan Malaysia, 43600 UKM Bangi, Selangor, Malaysia
[2]Research Center for Advanced Materials, National Research and Innovation Agency (BRIN), Building 224, KST BJ Habibie, South Tangerang 15314, Banten, Indonesia
[3]Department of Chemical Sciences, Faculty of Science and Technology, Universiti Kebangsaan Malaysia, 43600 UKM Bangi, Selangor, Malaysia

Received: 16 January 2023/Accepted: 25 July 2023

Abstract

TiO_2 nanotubes (NT) offer several advantages over other geometries for photoelectrochemical (PEC) applications. However, their performance in PEC water-splitting application has remained unsatisfactory due to its wide bandgap. To address this limitation, one approach is the incorporation of other materials as co-catalysts. Hence, in this study, a composite of TiO_2 NT and cobalt sulfide (Co_xS_y) was successfully synthesized, and its potential as a photoelectrode for water molecules splitting was evaluated. The TiO_2 NT was synthesized using electrochemical anodization of Ti foil, followed by annealing at 500 °C. Subsequently, Co_xS_y was added to the TiO_2 NT using hydrothermal method, and the composite was further annealed at 400 °C. Characterization technique, such as FESEM and XRD were employed to identify the morphological and phase structures, while UV-Vis reflectance spectroscopy was used for optical analysis. The efficiency of Co_xS_y deposited on to TiO_2 NT were evaluated by measuring the photocurrent generation. Remarkably, the sample of 60_Co_xS_y/TiO_2 NT exhibited photocurrent as high as 0.375 mA/cm^2 which is over sixfold higher than the bare TiO_2 NT. The results reported in this study were higher than those reported previously.

Keywords: Anodization; cobalt sulfide; co-catalyst; photocurrent density; TiO_2 NT

Abstrak

TiO_2 nanotiub (NT) menawarkan beberapa kelebihan berbanding geometri lain untuk aplikasi fotoelektrokimia (PEC). Walau bagaimanapun, prestasinya dalam aplikasi pembelahan molekul air PEC masih tidak memuaskan disebabkan sela jalurnya yang luas. Untuk mengatasi kekurangan ini, salah satu pendekatan adalah menambah bahan lain sebagai pemangkin bersama. Oleh itu, dalam kajian ini, komposit TiO_2 NT dan kobalt sulfida (Co_xS_y) telah berjaya sintesis dan keupayaannya sebagai fotoelektrod untuk pembelahan molekul air dinilai. TiO_2 NT disintesis menggunakan kaedah anodisasi foil Ti, diikuti penyepuhlindapkan pada 500 °C. Seterusnya, Co_xS_y ditambah kepada TiO_2 NT menggunakan kaedah hidroterma, diikuti dengan penyepuhlindapan pada 400 °C. Teknik pencirian, seperti FESEM dan XRD digunakan untuk mengenal pasti struktur morfologi dan fasa, manakala spektroskopi pemantulan UV-Vis digunakan untuk analisis optik. Kecekapan pemendapan Co_xS_y ke atas TiO_2 NT dinilai dengan mengukur penjanaan fotoarus. Sampel 60_ Co_xS_y/TiO_2 NT mengeluarkan fotoarus setinggi 0.375 mA/cm^2 yang lebih enam kali ganda lebih tinggi daripada TiO_2 NT tulen. Hail kajian ini dilaporkan Keputusan yang dilaporkan lebih tinggi daripada yang dilaporkan sebelum ini.

Kata kunci: Anodisasi; ketumpatan arus foto; kobalt sulfida; pemangkin bersama; TiO_2 NT

INTRODUCTION

Hydrogen (H_2) is the most abundant element in the universe and has the potential as a future energy carrier to replace fossil fuels. H_2 reacts with oxygen (O_2) in a fuel cell electrochemical system to produce electricity with pure water as the only byproduct, thereby, this

technology is a clean and environmentally friendly method to produce electricity. The utilization of H_2 as fuel has started since the beginning of this century, primarily for powering spaceship (Brey et al. 2017; IRENA 2019). However, H_2 rarely available naturally as H_2 gas on earth, thus it needs to be extracted from various sources, such as hydrocarbon, water, acids, or bases substances. Among these sources, water molecules stand out as the most promising H_2 source due to their abundance and affordability. However, the process to extract H_2 from water molecules demands high energy, approximately ~237.2 KJ/mol. Therefore, the use of energy from renewable and sustainable sources becomes imperatives. Solar light energy, being abundant, available everywhere and free, emerges as the preferred renewable energy for water splitting.

There are two methods of water splitting with solar light energy, first is conventional approach that known as photovoltaic- electrolyzer (PV-Electrolyzer), where the process comprises two steps: electricity generation through PV and water electrolysis using PV-generated electricity. The second method is through direct photoelectrochemical (PEC) cell, in which the system is in one compact package. The solar light is directly exposed to the photoactive electrode material that immersed in a water solution (Chowdhury 2012). Compared to PV-Electrolyzer method, PEC water splitting requires lower current densities and exhibits higher electrolysis efficiencies, making it a highly sought-after approach for H_2 production.

The PEC method requires a photoelectrode based on semiconductor materials. Numerous semiconductor materials have been investigated for this purpose, including copper oxide (Cu_2O) (Salehmin et al. 2018), tungsten (VI) oxide (WO_3) (Ng et al. 2018), zink oxide (ZnO) (Bagal et al. 2022), cobalt oxide (Co_3O_4) (Moridon et al. 2019), and molebdenum disulfide (MoS_2) (Moridon et al. 2022). However, no single semiconductor has proven to be an ideal photoelectrode due to issues with charge separation and stability. Therefore, modifications to the materials are necessary, such as by surface modification, electronic modifications through doping and composites with other materials, adding dye-sensitizer molecules, or incorporating co-catalyst materials. Among the materials studied as a photoelectrode, TiO_2 is the first and remains widely investigated until today. TiO_2 is photoactive and has good chemical and photochemical stability, abundant availability on earth, and non-toxicity. However, its efficiency for PEC water splitting is very low because TiO_2 possesse a wide band gap (3.0–3.2 eV), allowing it to absorb only ultraviolet (UV) energy and not visible light energy. This restricts its ability to utilize a broader spectrum of light energy, thereby limiting its efficiency for PEC water molecule splitting application.

Various efforts have been made to improve the TiO_2 performance, including surface modifications and the use of nano-sized materials such as nanotubes (NT), nanoparticles (NP), and nanorods (NR). These approaches aim to increase the active sites of the redox reaction, thereby enhancing the water-splitting efficiency of PEC (Arifin, Daud & Kassim 2013). Additionally, the incorporation of other material as co-catalysts also has been widely reported. These co-catalyst plays crucial role in suppressing rapid charge recombination, thus significantly enhancing the activity and stability of the system. One type of co-catalysts of pure metals like Pt, which can induce a plasmonic resonance effect in the TiO_2 photocatalyst. This effect facilitates a continuously flow e^- to the conduction band (CB) of TiO_2, subsequently transferring them to the cathode (Etacheri et al. 2015). Another effective co-catalyst is a semiconductor, such as CdS which forms a heterojunction with TiO_2. This junction provides a site for exciting e^- of TiO_2 that do not reach the CB, thereby reducing their recombination rate with holes (h•). As a result, the valence band (VB) of TiO_2 remains filled by h•, promoting the oxidation reaction water molecules (Zhang et al. 2015). The combination of TiO_2 NR with CdS has been reported to increase the photocurrent density and stability nearly threefold to TiO_2 NR alone (Diby et al. 2019). In addition to CdS, cobalt sulfide is an intriquing co-catalyst worthy of investigation (Agustina et al. 2022). Cobalt has demonstrated high efficiency as an electrocatalysts in electrochemical water splitting. Moreover, cobalt metal-based materials are abundant, cost effective and non-toxic, making them environmentally friendly options.

Here, we present and evaluate the performance of cobalt sulfide as a co-catalyst to TiO_2 NT as photoelectode for water splitting. The TiO_2 NT is synthesized through an electrochemical anodization process of Ti-foil, while cobalt sulfide is deposited into the TiO2 NT using a hydrothermal method. Due to the various oxidation states of Co metal, the resulting cobalt sulfide is expected to exist in multiple phases, depending on annealing temperature such as CoS, CoS_2, Co_9S_8, Co_3S_4, and $Co_{1-x}S$ (Xu et al. 2016). Based on our previous study, we found that the optimal photocurrent density was achieved when cobalt sulfide was annealed at 400 °C for 2 h with Co_9S_8 as majority of phase (Rambey et al. 2020). The combination of these materials expected to

contribute significantly to development of more efficient photocatalytic systems.

Materials and Methods

Materials

The titanium foil (99.6% purity) with a thickness of 0.1 mm, nitric acid (HNO_3), thiourea (CH_4N_2S), and cobalt (III) nitrate ($Co(NO_3)_3.6H_2O$ from Sigma Aldrich. Etilena glikol (EG) and ammonium fluoride (NH_4F) from Merck, and deionized water. All chemicals were analytical grade and used as received.

Syntesis of TiO_2 NT photoelectode

Before anodization, a 3 × 2 cm^2 piece of Ti foil was immersed in 1 M HNO_3 for 15 minutes to enhance the oxide layer on the surface of Ti metal sheets. It was then rinsed with deionized water and dried in a stream of nitrogen. The anodization process of the Ti-foil was carried out using a two-electrode system connected to a power supply (Agilent, E3645A). In this system, a Ti sheet serve as the anode, and a Pt as the cathode. The electrolytes used consisted of 0.5 wt% NH_4F in EG solution with 3 vol% water. All anodization procedures were conducted at room temperature.

The first anodization process was performed at a potential of 60 V for 5 min, resulting in the formation of NT layer. Subsequently, the NT layer was ultrasonically removed using deionized water. Afterward, the same Ti foil underwent a second anodization process at 60 V for 30 min to produce a uniform TiO_2 NT layer. After two-step anodization, the prepared TiO_2 NT samples were cleaned with deionized water and dried with nitrogen gas. Next, TiO_2 NT was annealed at 500 °C for 1 hour with a ramping rate of 5 °C min^{-1}.

Syntesis CoS/TiO_2 NT

Here, CoS was deposited on the surface of TiO_2 NT using the hydrothermal method in a Teflon-coated stainless-steel autoclave with a capacity of 25 mL. The process involved dissolving 1.46 g of Co $(NO_3)_3.6H_2O$ in 8 mL of deionized water and stirring the solution for 30 min. Subsequently, 8 mL of an aqueous solution containing 0.38 g of CH_4N_2S was added dropwise to the mixture. After 30 min of stirring, the mixture was then transferred to a Teflon-lined stainless-steel autoclave, and the TiO_2 NT on the foil was placed with the TiO_2 side touching the solution.

The autoclave was then placed in a furnace, and the temperature was maintained at 180 °C for several time variations, namely 30 min and 60 min. Afterward, the autoclave was allowed to cool to room temperature and the foil washed several times with deionized water. It was then heated in an oven at 60 °C for 12 h, followed by annealling at 500 °C for 2 h. Overall synthesis processes in this study as shown in Figure 1.

Structural characterizations

The surface morphology, cross-section, and elemental composition of the samples were characterized using Field-emission scanning electron microscopy (FESEM; ZEISS Merlin) To identify the crystal structure, X-ray

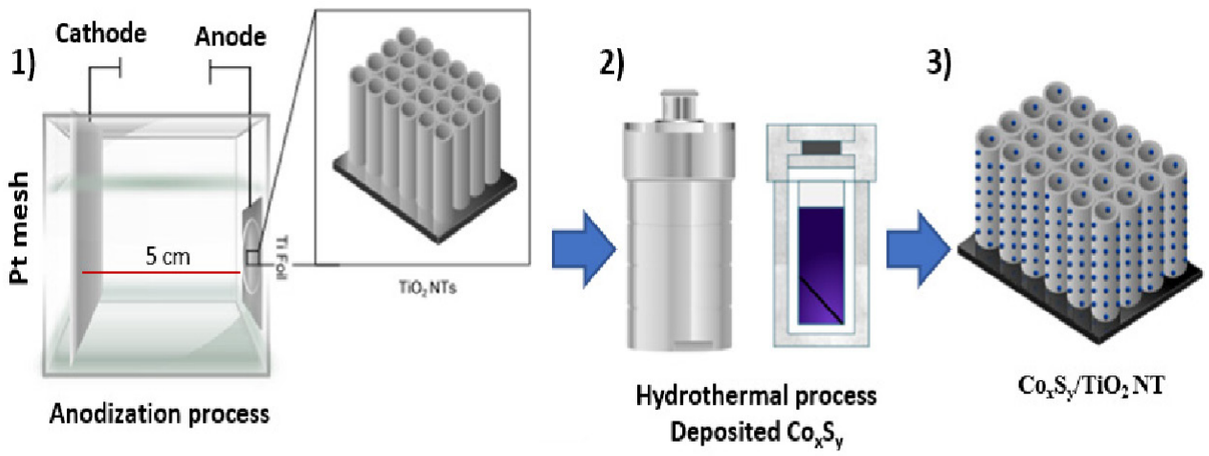

FIGURE 1. Schematic synthesis of Co_xS_y/TiO_2 NT:1) anodization Ti foil, (2) hydrothermal process

diffraction (XRD) was conducted on a Bruker D8 Discover diffractometer using Cu Ka radiation (1.540 598 Å). Additionally, the optical properties of the samples was studied using a UV-Vis-NIR spectrophotometer (Perkin Elmer, Lambda 950).

PEC MEASUREMENT

The PEC water-splitting analysis was performed using a designed photocell with an exposed area of 1 cm^2 using a PGSTAT 302N Autolab Potentiostat/Galvanostat (Metrohm) equipped with a three-electrode system. The thin working electrodes was a thin film, while a platinum wire served as the a counter electrode, and an Ag/AgCl electrode was used as the reference electrode. To measure the photocurrent density, linear sweep voltammetry (LSV) was employed in two condition; in dark and under light irradiations. The scan rate for LSV was set at $5mVs^{-1}$. The light irradiation was conducted by using a Xe 300W lamp (PLS-SXE300, PE300BF) equipped with a 1.5G AM filter. To ensure accurate light source intensity, the lamp was calibrated with Si diode (Model 818, Newport) to simulate 1.5G AM lighting at intensity of 100 mW/cm^2.

RESULTS AND DISCUSSIONS

CHARACTERIZATION AND PEC MEASUREMENT OF TiO_2 NT

The performance of TiO_2 NT in PEC water splitting is influenced by various factors, including the nanotubes length, wall thickness, tube diameter, and spacing between the tubes. These morphological characteristics are crucial in determining the overall efficiency. Anodization time is one of factor that play a significant role in this process (Ozkan et al. 2018). Here, the TiO_2 NT produced by three variations of anodization times was carried out. Prior to the anodization process, the Ti-foil was pre-treated with HNO_3 to enhance the oxide layer on its surface, which facilitated the formation of NTs (Indira et al. 2015). Figure 2 shows the morphology of Ti foil before and after 15 min etching process. Notably, the surface of Ti metal after etching exhibited a thicker oxide layer compared to pre-etching, as evidenced by its coarser apperance. The treated Ti foil was thoroughly rinsed with deionized water to remove any remaining acid before proceeding with anodization process.

Figure 3 are the FESEM images of the surface and cross-section morphology of TiO_2 NTs under three anodization times, that is 30 min, 1 h, and 2 h. When anodized for 30 min, the growth of NTs resulted in noticeable distance between each tube, leading to less robust NTs structures. The pore diameter of the produced NTs is remarkably uniform with average diameter of 123 nm, while the thickness produced is ~2 µm. At 1 h of anodization, the TiO_2 NT produced exhibits a higher level of regularity, characterized by thicker tube wall and narrow spacing between tubes compared to those produced at 30 min. Meanwhile, the diameter and height of the NT produced were 126 nm and 2.9 µm, respectively. Upon extending the anodization process to 2 hours, the morphology of the resulting NTs undergoes a transformation, with an average length reaching ~4.2 µm and an average diameter of 154.8 nm.

Figure 4 displays the XRD results of the TiO_2 NT samples anodized for 30 min, 1 h and 2 h, showing the presence of both the anatase and rutile phase. The diffraction peak in TiO_2NT samples occurred at 25.8º

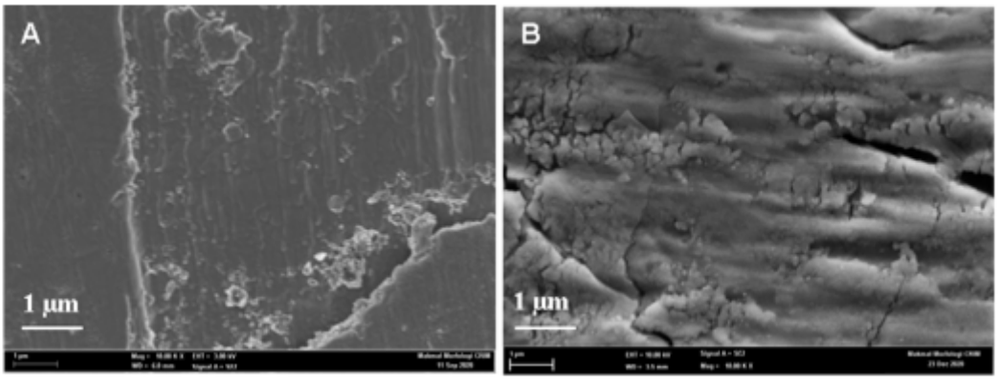

FIGURE 2. FESEM of (A) Ti sheets before and (B) after treated with HNO_3

(anatase), 27.4º (rutyl), 36.1º (rutile), 37.8º (anatase), 38.6º (anatase), 41.3º (rutyl), 48 º (anatase), 53.9 (Anatase) and 55.1º (anatase). These results indicated that TiO_2 NT with an annealing temperature of 500 ºC for 1 h was a mixture of anatase and rutile (JCPDS No. 21-1272).

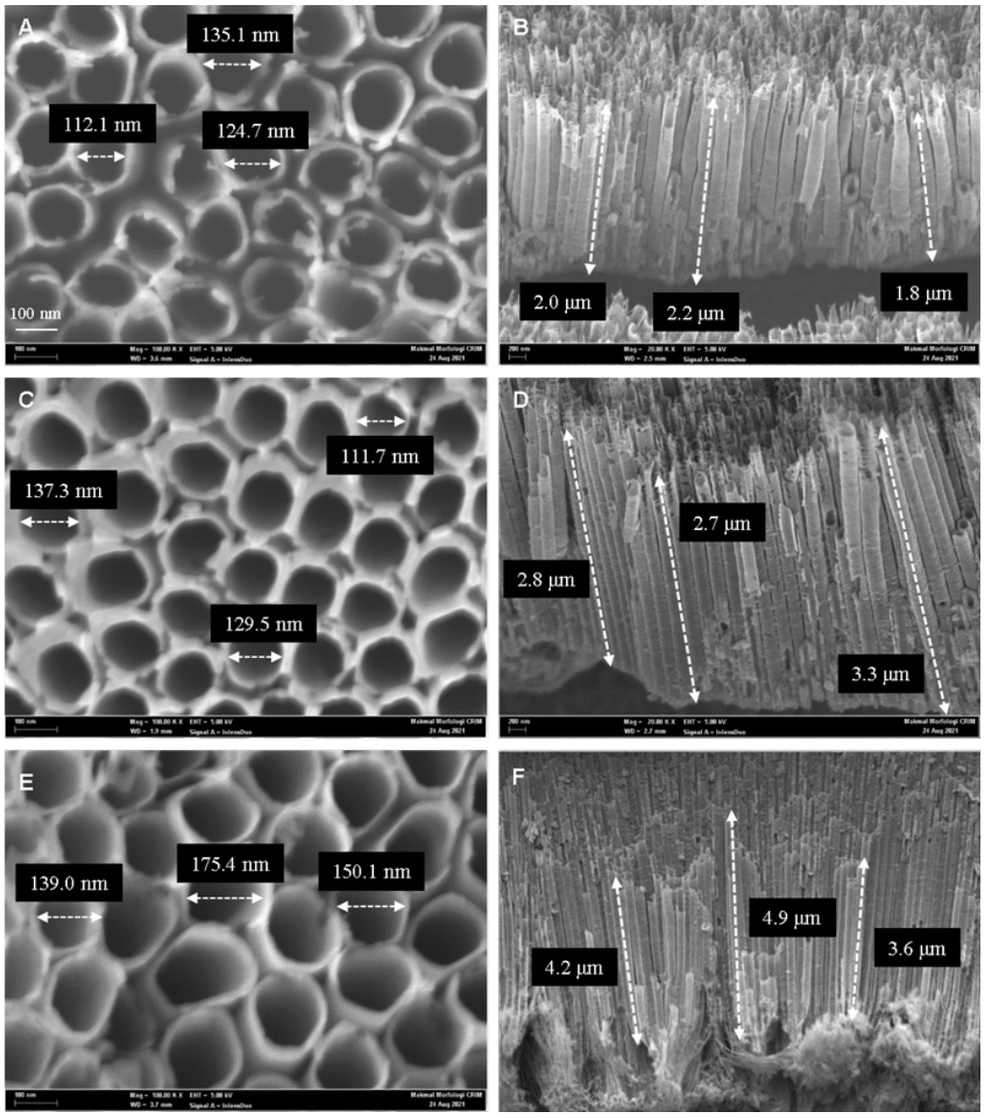

FIGURE 3. FESEM of (A&B) TiO_2 NT surface and cross section after 30 min anodization; (C&D) TiO_2 NT surface and cross section after 1 h anodization, (E&F) TiO_2 NT surface and cross section after 2 h anodization process

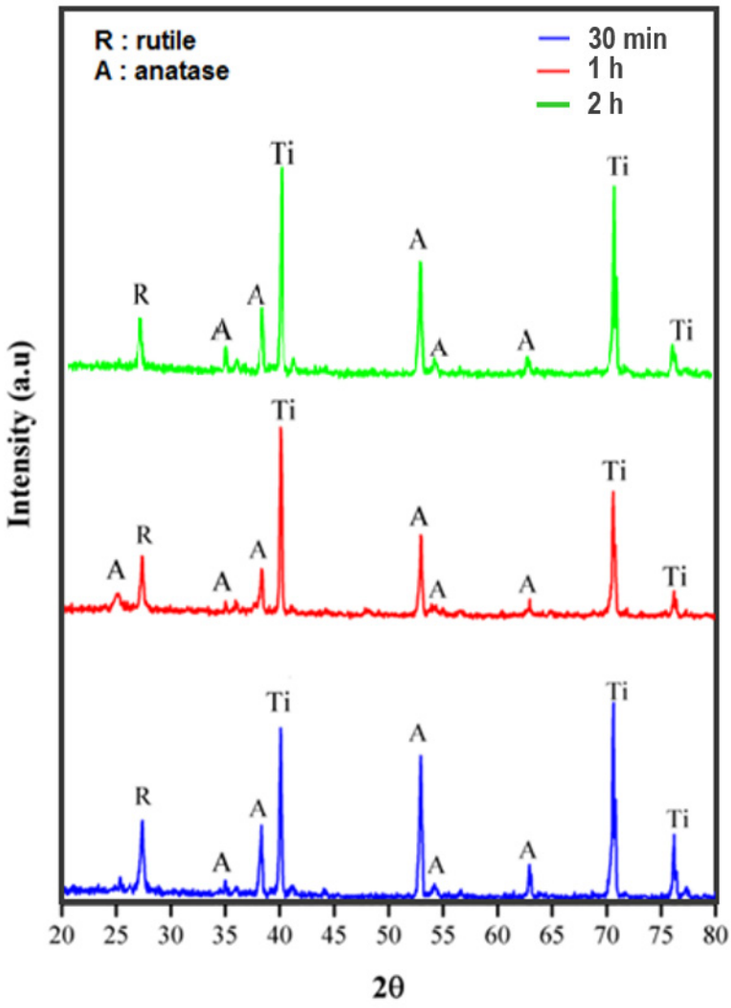

FIGURE 4. Spektrum XRD TiO_2 NT produced after 30 min, 1 h and 2 h anodization process

The photoelectrochemical (PEC) performance of TiO_2 NT resulting from anodization at these three different anodization times was evaluated on the photocurrent density. Figure 5 illustrates the current curve (I – V) obtained under both dark and light conditions. The photocurrent densities for samples anodized for 30 min, 1 h and 2 h were measured as 154 μA/cm^2, 90 μA/cm^2, and 92 μA/cm^2, respectively, at applied potential of 1.0 V. Among the various anodization times, the highest photocurrent density was observed in the 30 min anodized sample. It is hypothesized that the increased intertube spacing in the NTs resulting in 30 min anodization might have contributed to this enhancement. The presence of intertube spacing plays a crucial role in influencing the PEC performance by promoting charge transfer and light absorption properties of the NTs (Arifin, Daud & Kassim 2013). However, despite this improvement, the overall performanceof the PEC cell remained relatively low. To address this limitation, the study proposed the incorporation of the other species as co-catalyst to potentially enhance the overall performance (Moridon et al. 2022). Furthermore, the addition of cobalt sulfide to the 30 minutes anodization sample via hydrothermal method was investigated.

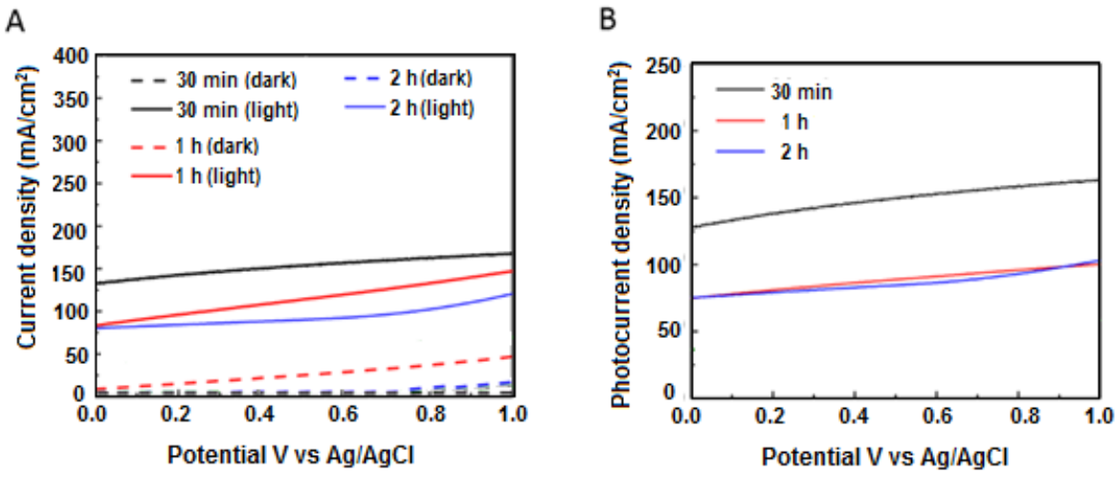

FIGURE 5. PEC measurements of TiO_2 NT analyzed at an annealing temperature of 500 ºC with variations in anodization time of 30 min, 1 h and 2 h

CHARACTERIZATION AND PEC MEASUREMENT OF COS DOPED-TiO_2 NT

TiO_2 NT were produced through a 30 min anodization process, subsequently combined with cobalt sulfide using two different hydrothermal reaction times. Figure 6 shows the FESEM images of Co_xS_y/TiO_2 obtained after 30 min (a) & 60 min (b) of the hydrothermal process. At sample of 30 minutes of hydrothermal reaction (30_Co_xS_y/TiO_2), Co_xS_y began to grow in a small amount, forming a cotton-like shape, and was not completely covered on the surface of TiO_2 NT. However, after 60 min of hydrothermal reaction (60_Co_xS_y/TiO_2), the deposition of Co_xS_y increased significantly and it become more densely and uniformly dispersed on the surface of TiO_2 (Figure 6(a1) & 6(b1). The similar morphology is consistent with the findings that has been reported by Yu et al. (2014). The presence of Co, S, Ti, and O elements on both samples were confirmed by EDX results. Content of Co on 60_Co_xS_y/TiO_2 sample was found higher compared in 30_Co_xS_y/TiO_2 sample (Figure 6(a2) -6(a3), meanwhile sulfur content reverse. Percentage sulfur at sample 60_Co_xS_y/TiO_2 (Figure 6(b2) -6(b3), was found lower then in 30_Co_xS_y/TiO_2. The atomic ratio of Co:S approximately are 2.1 and 10:1 indicates the phases of Co_xS_y in both samples probably is Co_9S_8, with a wide deviation. This discrepancy in elemental content may be attributed by incomplete cleaning after hydrothermal process.

Figure 7 shows a comparative XRD pattern between TiO_2 NT 30 min anodized, CoxSy powder and 30_Co_xS_y/TiO_2. In the XRD pattern, distinct peaks are observed at 33.50º, 47º, and 54.32º which are denoted as (100), (102), and (110) of the cobalt sulfide crystal plane (JCPDS no. No. 65-8977). Based on our previous study, the cobalt sulfide is a temperature-dependent material, in which the cobalt sulfide annealed at 400 °C for 2 h produced mixed phases with majority phase is C_9S_8 phase which produced the optimal photocurrent density (Rambey et al. 2020). Meanwhile, peaks TiO_2 appear at 25.8º (anatase), 27.4º (rutile), 36.1º (rutile), 37.8º (anatase), 38.6º (anatase), 41.3º (rutyl), 48 º (anatase), 53.9 (Anatase) and 55.1º (anatase). Notably, the peak at 25.8º exhibited the highest intensity among other peaks, confirming that the anatase is the dominant phase in the TiO_2 NT. Here, we only analyzed sample of 30_Co_xS_y/TiO_2, with a lowest content of Co_xS_y, as representative to confirm presence of Co_xS_y on both samples.

The UV-Vis absorption of TiO_2 NT and Co_xS_y/TiO_2 NT samples is depicted in Figure 8(A). All samples demonstrated high absorption in UV spectrum between 370-420 nm, which is a characteristic of TiO_2 absorption. Furthermore, the 60_Co_xS_y/TiO_2 NT sample exhibits stronger absorption in the visible light region around 600 nm compared to both pure TiO_2 NT and Co_xS_y/TiO_2 NT. This strong absorption is likely attributed to the presence of an adequate amount of Co_xS_y in the composite. The optical bandgap can be calculated using Tauc Plot as $(ah\nu)^{n/2} = h\nu - Eg$, where n is equal to 1 for a direct bandgap calculation. Figure 8(B) illustrated the relationship between $(ah\nu)^{1/2}$ and $h\nu$. The 60_Co_xS_y/TiO_2

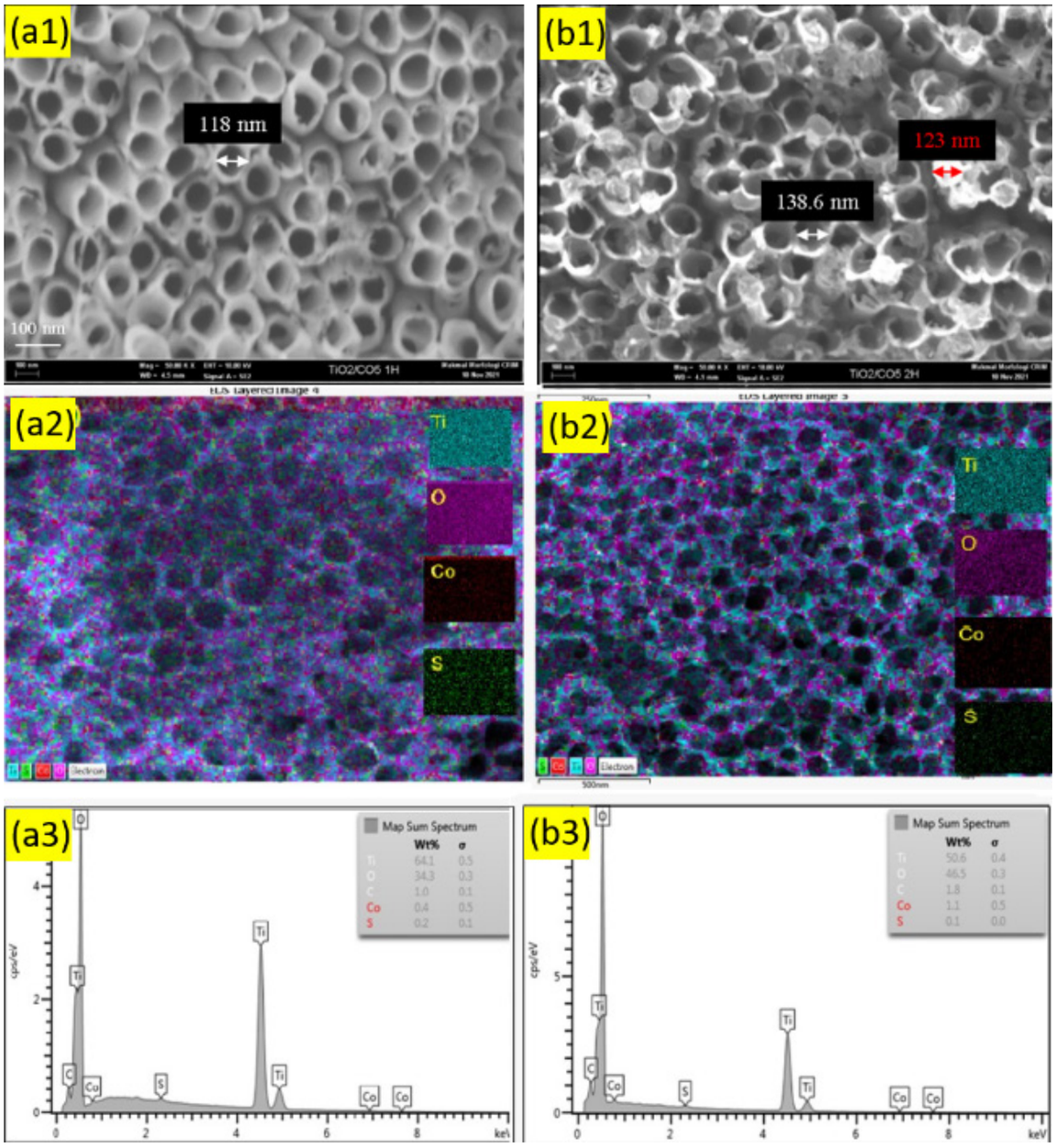

FIGURE 6. FESEM images of surface morphology, mapping and EDX spectra of (a) 30_Co_xS_y/TiO_2 NT and (b) 60_Co_xS_y/TiO_2 NT samples

NT sample exhibits the lowest bandgap at approximately 1.5 eV. This bandgap in line with the strong absorption on visible light region. On the other hand, the 30_Co_xS_y/TiO_2 NT sample shows a bandgap of 1.7 eV, lowe than pure TiO_2 NT bandgap of 2.3 eV. The results of the optical bandgap in this study are lower than previous reported bandgap value (Agustina et al. 2022; Liu et al. 2017).

Figure 9(A) and 9(B) illustrates the LSV results of TiO_2 NT and Co_xS_y/TiO_2 NT obtained through 30 min and 60 min hydrothermal reactions, in 1 M KOH solution. The photocurrent density of all samples demonstrated an increase with rising voltage up to with 0.35 V. Beyond this point, the initial current density decreased and then the starting current density decreased for 60_CoS/

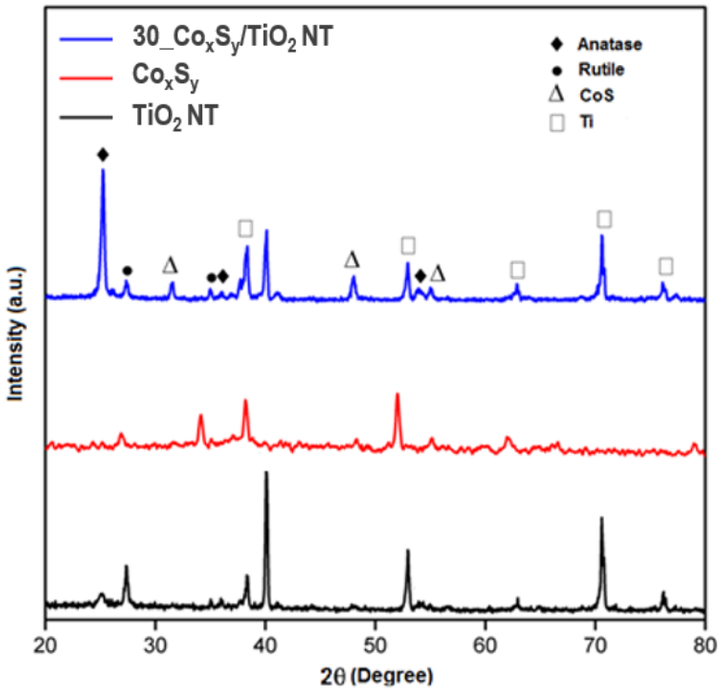

FIGURE 7. XRD spectrum comparison between sample of 30_ Co_xS_y/TiO_2 NT, CoS powder and TiO_2 NT

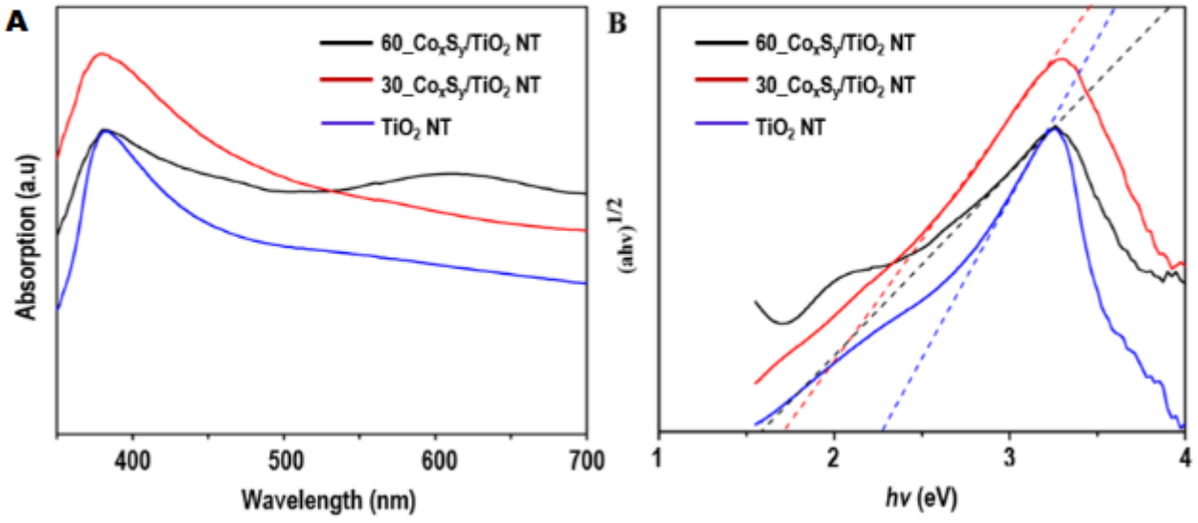

FIGURE 8. (A) Spectrum absorption, and (B) Tauc plot of TiO_2 NT and Co_xS_y/TiO_2 NT samples

TiO_2 NT samples. This phenomenan may be attributed to one of the drawbacks of metal sulfides, particularly their susceptibility to photocorrosion, rendering them unstable in specific electrolyte atmospheres (Moridon et al. 2022). The measured photocurrent density of TiO_2 NT photoanode is 0.05 mA/cm^2 (vs. Ag/AgCl). However, there is no significant increase in photocurrent density with an increase in applied voltage. Notably, both samples

of Co_xS_y/TiO_2 NT exhibited higher photocurrent density than pure TiO_2 NT. Specifically, the 60_ CoS/TiO_2 NT sample produced the highest photocurrent density of 0.375 mA/cm^2 at 0.35 V vs Ag/AgCl, surpassing TiO_2 NT by is over sixfold. On the other hand, the 30_Co_xS_y/TiO_2 NT sample achieved a photocurrent density of 0.2 mA/cm^2 at potential of 0.35 V, which is lower than 60_ CoS/TiO_2 NT sample. The lower photocurrent density observed in the 30_ Co_xS_y/TiO_2 NT sample was may be attributed to the limited amount of Co_xS_y deposited on the surface. Despite this, the photocurrent density displays a discernible increasing trend up to a voltage 0.4 V vs Ag/AgCl. Notably, the results obtained in this study surpass those reported by Liu et al. 2017 (Table 1).

Figure 9(C) depicts the typical Nyquist plots of TiO_2-NT and 60_ Co_xS_y/TiO_2 NT sample. As observed, the Co_xS_y/TiO_2 NT photoanode exhibits a smaller curve compared to the TiO_2 NT photoanode, indicating that the incorporation of Co_xS_y into the TiO_2 photoanode enhances the separation of photo-generated electron-hole pairs and facilitates charge transport. The reduces charge transfer resistance in Co_xS_y/TiO_2 NT photoanodes can be attributed to the improved conductivity and electron mobility achieved by introducing Co_xS_y . The Mott-Schottky plots (Figure 8(D)) of both TiO_2-NT and 60_ Co_xS_y/TiO_2 NT samples display a positive slop, indicating that it behave as an n-type semiconductor with electrons as the majority carriers. Co_xS_y on TiO_2 NT photoanodes can synergistically affect electron transfer, further enhancing charge isolation, This effect leads to a greater number of holes participating in photoelectrochemical water oxidation.

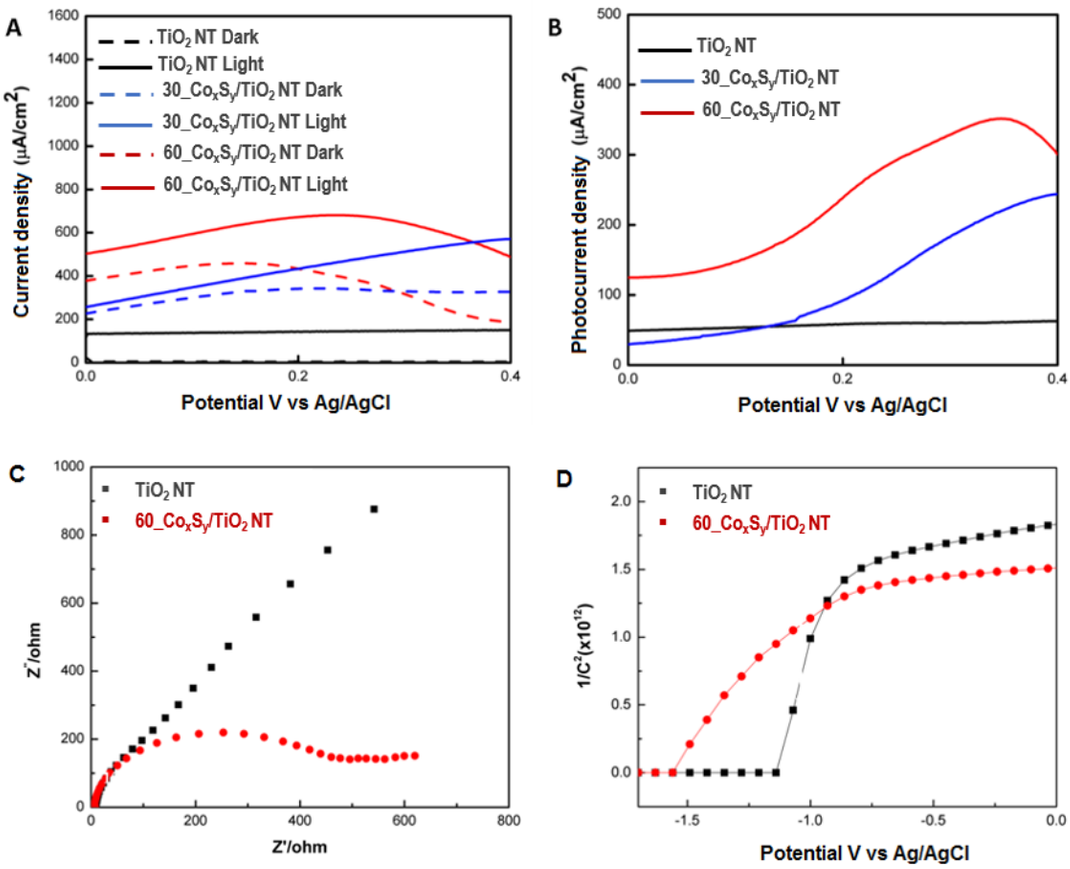

FIGURE 9. (A,B) LSV, (C) EIS and (D) Mott Schottky of TiO_2 NT and Co_xS_y/TiO_2 NT composite with hydrothermal time variations

TABLE 1. Performance results and parameters compared with other studies

Parameter	Previous study reported		This study
	Liu et al. (2017)	Agustina et al. (2022)	
Samples	Co_9S_8/TiO_2 NT	CoS/TiO_2 powder	Co_9S_8/TiO_2 NT
Photocurrent density	0.25 mA/cm^2 at potential of 0.35 V	0.134 mA/cm^2 at potential of 0.35 V	0.375 mA/cm^2 at potential of 0.35 V
Bandgap	3.1 eV	2.75 eV	1.5 eV
Electrolyte	0.5 M Na_2SO_4	0.5 M Na_2SO_4	1 M KOH

Conclusion

Composites of Co_xS_y on TiO_2 NT have been evaluated as a photoanode for PEC water oxidation and have demonstrated superior performance compared to bare TiO_2 NT. The photocurrent density of the composite photoanode is 0.375 mA/cm^2 (at 0.35 V vs. Ag/AgCl), which is a sixfold higher than that of TiO_2 NT. The significant improvement in photocatalytic performance can be attributed to the synergistic effect of simplified charge separation and favorable electron transport facilitated by Co_xS_y . Furthermore, the Mott-Schottky plot confirms that Co_xS_y/TiO_2-NT composites as efficient photoanodes for PEC water splitting applications.

Acknowledgements

This research was funded by the Malaysian Ministry of Higher Education (MOHE) under Research Grant FRGS/1/2020/STG04/UKM/02/5.

References

Agustina, M., Moridon, S.N.F., Linggawati, A., Arifin, K., Minggu, L.J. & Kassim, M.B. 2022. Hydrogen production from water splitting using TiO_2/CoS composite photocatalyst. *Sains Malaysiana* 51(10): 3251-3259.

Arifin, K., Daud, W.R.W. & Kassim, M.B. 2013. Optical and photoelectrochemical properties of a TiO2 thin film doped with a ruthenium–tungsten bimetallic complex. *Ceramics International* 39(3): 2699-2707.

Bagal, I.V., Arunachalam, M., Abdullah, A., Waseem, A., Kulkarni, M.A., Kang, S.H. & Ryu, S-W. 2022. Toward stable photoelectrochemical water splitting using NiOOH coated hierarchical nitrogen-doped ZnO-Si nanowires photoanodes. *Journal of Energy Chemistry* 71: 45-55.

Brey, J., Muñoz, D., Mesa, V. & Guerrero, T. 2017. Use of fuel cells and electrolyzers in space applications: From energy storage to propulsion/deorbitation. *E3S Web of Conferences* 16: 17004. DOI: 10.1051/e3sconf/20171617004

Chowdhury 2012

Diby, N.D., Duan, Y., Grah, P.A., Cai, F. & Yuan, Z. 2019. Enhanced photoelectrochemical water-splitting performance of TiO_2 nanorods sensitized with CdS via hydrothermal approach. *Journal of Alloys and Compounds* 803: 456-465.

Etacheri, V., Di Valentin, C., Schneider, J., Bahnemann, D. & Pillai, S.C. 2015. Visible-light activation of TiO_2 photocatalysts: Advances in theory and experiments. *Journal of Photochemistry and Photobiology C: Photochemistry Reviews* 25: 1-29.

Indira, K., Mudali, U.K., Nishimura, T. & Rajendran, N. 2015. A review on TiO_2 nanotubes: Influence of anodization parameters, formation mechanism, properties, corrosion behavior, and biomedical applications. *Journal of Bio- and Tribo-Corrosion* 1(4): 28.

IRENA. 2019. *Hydrogen: A Renewable Energy Perspective.* International Renewable Energy Agency, Abu Dhabi.

Liu, R., Sun, Z., Song, X., Zhang, Y., Xu, L. & Xi, L. 2017. Toward non-precious nanocomposite photocatalyst: An efficient ternary photoanode TiO_2 nanotube/Co_9S_8/polyoxometalate for photoelectrochemical water splitting. *Applied Catalysis A: General* 544: 137-144.

Moridon, S.N.F., Arifin, K., Yunus, R.M., Minggu, L.J. & Kassim, M.B. 2022. Photocatalytic water splitting performance of TiO_2 sensitized by metal chalcogenides: A review. *Ceramics International* 48(5): 5892-5907.

Moridon, S.N.F., Salehmin, M.I., Mohamed, M.A., Arifin, K., Minggu, L.J. & Kassim, M.B. 2019. Cobalt oxide as photocatalyst for water splitting: Temperature-dependent phase structures. *International Journal of Hydrogen Energy* 44(47): 25495-25504.

Ng, K.H., Minggu, L.J., Mark-Lee, W.F., Arifin, K., Jumali, M.H.H. & Kassim, M.B. 2018. A new method for the fabrication of a bilayer WO_3/Fe_2O_3 photoelectrode for enhanced photoelectrochemical performance. *Materials Research Bulletin* 98: 47-52.

Ozkan, S., Nguyen, N.T., Mazare, A. & Schmuki, P. 2018. Optimized spacing between TiO_2 nanotubes for enhanced light harvesting and charge transfer. *ChemElectroChem* 5(21): 3183-3190.

Rambey, M.A., Arifin, K., Minggu, L.J. & Kassim, M.B. 2020. Cobalt sulfide as photoelectrode of photoelectrochemical hydrogen generation from water. *Sains Malaysiana* 49(12): 3117-3123.

Salehmin, M.N.I., Minggu, L.J., Mark-Lee, W.F., Mohamed, M.A., Arifin, K., Jumali, M.H.H. & Kassim, M.B. 2018. Highly photoactive Cu_2O nanowire film prepared with modified scalable synthesis method for enhanced photoelectrochemical performance. *Solar Energy Materials and Solar Cells* 182: 237-245.

Xu, Q., Jiang, D., Wang, T., Meng, S. & Chen, M. 2016. Ag nanoparticle-decorated CoS nanosheet nanocomposites: A high-performance material for multifunctional applications in photocatalysis and supercapacitors. *RSC Advances* 6(60): 55039-55045.

Yu, Z., Meng, J., Xiao, J., Li, Y. & Li, Y. 2014. Cobalt sulfide quantum dots modified TiO_2 nanoparticles for efficient photocatalytic hydrogen evolution. *International Journal of Hydrogen Energy* 39(28): 15387-15393.

Zhang, H., Zhang, D., Qin, X. & Cheng, C. 2015. Three-dimensional CdS-Sensitized sea urchin like TiO_2-ordered arrays as efficient photoelectrochemical anodes. *The Journal of Physical Chemistry C* 119(50): 27875-27881.

*Corresponding author; email: khuzaim@ukm.edu.my